Nabi, Md. Nurun; Hustad, Johan Einar; Arefin, Md. Arman

Article

The influence of Fischer-Tropsch-biodiesel-diesel blends on energy and exergy parameters in a six-cylinder turbocharged diesel engine

Energy Reports

Provided in Cooperation with:
Elsevier

Suggested Citation: Nabi, Md. Nurun; Hustad, Johan Einar; Arefin, Md. Arman (2020) : The influence of Fischer-Tropsch-biodiesel-diesel blends on energy and exergy parameters in a six-cylinder turbocharged diesel engine, Energy Reports, ISSN 2352-4847, Elsevier, Amsterdam, Vol. 6, pp. 832-840,
https://doi.org/10.1016/j.egyr.2020.04.011

Energy Reports 6 (2020) 832–840

Contents lists available at ScienceDirect

Energy Reports

journal homepage: www.elsevier.com/locate/egyr

Research paper

The influence of Fischer–Tropsch-biodiesel–diesel blends on energy and exergy parameters in a six-cylinder turbocharged diesel engine

Md Nurun Nabi [a,*], Johan Einar Hustad [b], Md Arman Arefin [c]

[a] School of Engineering and Technology, Central Queensland University, Perth, WA 6000, Australia
[b] Department of Energy and Process Engineering, Norwegian University of Science and Technology, Norway
[c] Department of Mechanical Engineering, Rajshahi University of Engineering & Technology, Rajshahi, Bangladesh

ARTICLE INFO

Article history:
Received 28 November 2019
Received in revised form 30 March 2020
Accepted 4 April 2020
Available online xxxx

Keywords:
Energy
Exergy
Fischer–Tropsch fuel
Jatropha biodiesel
Oxygen ratio

ABSTRACT

This investigation explores the influence of oxygenated fuels on different energy and exergy parameters first and the second law of thermodynamics. The parameters were estimated based on the experimental data using thermodynamic Equations. Due to similar fuel properties to diesel, a Fischer–Tropsch fuel (FT100) was used as a base fuel (reference fuel) in the current investigation. Three biodiesel blends were prepared with Fischer–Tropsch fuel. Non-edible Jatropha biodiesel (*Jatropha curcas*) was selected to avoid food versus fuel conflict. All blends were prepared on a volumetric basis. The first blend was prepared using 25% of biodiesel and 75% of Fischer–Tropsch fuel and termed as B25. The second blend was made with 50% biodiesel and 50% Fischer–Tropsch fuel and designated as B50. The third and the final blend was formulated with 75% biodiesel and 25% Fischer–Tropsch fuel and abbreviated as B75. The three blends were also termed as oxygenated blends as they contain 3 wt%, 5.9 wt% and 8.7 wt%, respectively oxygen content in their molecule. Neat biodiesel (B100) was not targeted in this investigation. A new parameter "oxygen ratio" was used to make a correlation between different energy and exergy parameters with oxygen ratio. Instead of showing different energy and exergy parameters against equivalence ratio or excess air ratio, for better understanding, it is worth showing those parameters with oxygen ratio as all blends are inherently oxygenated. The results show almost insignificant variations in different parameters with the three oxygenated blends when compared to those of the FT100.

1. Introduction

A significant amount of work has been done on alternative and biofuels, as they are getting much interest nowadays as fuels for internal combustion engines (López et al., 2014; Nabi et al., 2013; Zare et al., 2017). Most of the research work focused on the influence of biofuels on engine performance, combustion and emissions (Nabi et al., 2019c,b,a; Nabi and Rasul, 2018; Rahman et al., 2015; Nabi and Hustad, 2012; Bodisco et al., 2019). Studies also were done on the effect of fuel properties on engine behaviour, including performance and emissions (Iqbal et al., 2015; Liu et al., 2013). Besides engine performance and emissions, some studies showed energy and exergy analysis with diesel and biofuels (López et al., 2014; Meisami and Ajam, 2015; Hoseinpour et al., 2017; Khoobbakht et al., 2016). The exergy is an important concept of probable estimation of irreversibilities linked with the process (López et al., 2014). Hoseinpour et al. (2017) did experimental investigation in diesel engine fuelling with diesel, diesel–biodiesel blends by fumigating gasoline. The authors reported different energy and exergy parameters including thermal efficiency, energy and exergy fractions for the neat diesel, diesel+gasoline fumigation, biodiesel+gasoline fumigation. They also reported that the maximum energy and exergy with biodiesel+gasoline fumigation were observed at high load. Ertunc Tat (2011) investigated the influence of cetane number as well as delay period on exergy and energy efficiencies fuelling with four methyl esters. The author concluded that exergy analysis is useful for optimising or correlating combustion parameters. Khoobbakht et al. (2016) did a similar investigation with diesel, ethanol and biodiesel blend. They studied the influence of engine load and speed on exergy efficiency. The authors also studied destruction exergy and thermal efficiency. Due to exergy destruction, the internal combustion engines show low efficiency (Hoseinpour et al., 2017). Ozcan (2010) did both experimental and computational investigations with hydrogen enrichment in a spark–ignition engine. The author studied the influence of hydrogen addition on different exergetic parameters, including fuel chemical exergy, total exergy, second-law efficiency. The

* Corresponding author.
E-mail address: m.nabi@cqu.edu.au (M.N. Nabi).

https://doi.org/10.1016/j.egyr.2020.04.011

author reported higher second-law efficiency with a higher percentage of hydrogen. The second-law efficiency was found to be higher near the lean limit. Besides exergy efficiency, López et al. (2014) also investigated unitary exergetic cost with neat diesel, neat biodiesel and diesel–biodiesel blends. The authors reported a slight difference in unitary cost for the tested blends and diesel fuel. The slight difference in unitary cost between diesel fuel and the blends was associated with the engine's fuel supply system and the combustion chamber design. Sayin Kul and Kahraman (2016) investigated energy and exergy with diesel, biodiesel and ethanol blends in a single cylinder diesel engine. The authors reported lower exergetic and thermal efficiency with the biodiesel blends compared to those of diesel fuel. Besides engine performance, emission and energy, Panigrahi et al. (2014) did analysis on exergy for the biodiesel 20% blend with 80% diesel (B20). They reported that diesel's input availability is higher by 1.46% compared to B20. The authors also reported that compared to B20, diesel also shows higher brake power availability and exhaust gases availability by 5.66% and 32% respectively. Exergy destruction with B20 was found to be 0.97% higher than diesel.

In the current study, exergy and energy calculations were conducted using three biodiesel blends and a neat Fischer–Tropsch fuel (FT100). Jatropha biodiesel was selected in the current investigation for avoiding the food versus fuel conflict. One of the key targets was to find the optimum biodiesel blend by comparing the different exergy and energy parameters with those of Fischer–Tropsch fuel. For the experiment, a direct injection, the six-cylinder diesel engine was chosen. In the analyses, a new parameter "oxygen ratio" was introduced to make a correlation between different energy, exergy parameters and oxygen ratio. The justification of choosing the parameter "oxygen ratio" is, the fuels tested in this investigation are oxygenated fuels, meaning the availability of oxygen in the fuel molecules. It has been revealed that no literature was found that dealt with energy and exergy parameters against oxygen ratio.

2. Materials and methods

All experimental measurements were done in a six-cylinder, turbocharged diesel engine. The key specifications of the engine are given in Table 1. All experiments were conducted at a constant engine speed of 1450 rpm. The speed was optimised based on engine thermal efficiency (Nabi et al., 2009). The dynamic fuel injection timing was set at 20 °CA BTDC. The engine was run at five different loads including 3%, 25%, 50%, 75% and 92% of full load. The detailed properties of the tested fuels can be found at (Nabi and Hustad, 2010; Nabi et al., 2009; Kannan et al., 2009). The different measuring instruments used for the measurement of gaseous emissions are as follows:

Instrument	Measured gaseous component
Horiba PG-250; Chemiluminescence detector (CLD)	NOx
JUM 3-200; Heated flame ionisation detector (FID)	Unburnt hydrocarbon
AVL 415S smoke metre	Filter smoke number (FSN)
ELPI, DEKATI	Particle number

The objectives of the current investigations are as follows:

- To investigate the energy and exergy parameters of biodiesel (oxygenated) blends and FT100.
- To compare the energy and exergy parameters of three biodiesel blends with those of FT100.

Table 1
Specifications of the test engine (Nabi and Hustad, 2012).

Engine type	Scania DC 1102
Cylinder (−)	6
Compression ratio (−)	18
Bore × Stroke (mm)	127 × 140
Peak torque @1080–1500 rpm (N m)	1750
Peak power @1800 rpm (kW)	280
Needle opening pressure (MPa)	22
Injection	Unit injector
Hole size (mm) × number (−)	ϕ 0.216 × 8

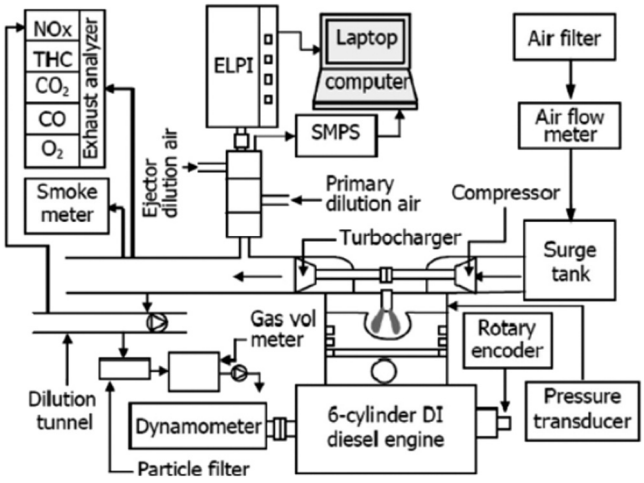

Fig. 1. Schematic of the experimental setup (Nabi et al., 2009).

2.1. Combustion analysis

In this study, the different emission components, including CO, O_2, CO_2, HC and NO were used. N_2, H_2O, and H_2 were obtained by balancing the chemical Equation using the measured components. Nitrogen dioxide (NO_2) and particulate matter (PM) were neglected in the analysis as their concentrations were sufficiently low. The generalised combustion Equation can be written in Eq. (1).

$$C_\alpha H_\beta O_\gamma + a(O_2 + 3.76N_2) \rightarrow bO_2 + cCO + dCO_2 + eNO + fNO_2 + gN_2 + hH_2O \quad (1)$$

where, a, b, c, d, e, f, g, h are the mole fractions of the individual emission components. It is supposed that no water vapour is present in the intake air, thus for simplicity taking 21% oxygen and 79% nitrogen in the air. Based on the air, fuel mass flow rate and measured exhaust gas concentrations, the unknown coefficients can be estimated (Canakci and Hosoz, 2006; Meisami and Ajam, 2015).

2.2. Oxygen ratio

This study uses a new terminology "oxygen ratio" (OR) instead of using excess air ratio or fuel air equivalence ratio. The justification of using the term oxygen ratio as the fuels are oxygenated and contain oxygen in their molecules. Pham et al. (2014) used the OR for several oxygenated fuels. The use of OR is more appropriate terminology for defining the stoichiometry of oxygenated fuels. The OR can be defined by Eq. (2) (Zare et al., 2016):

$$OR = \frac{Oxygen_{fuel+}\ Oxygen_{air}}{Stoichiometric\ oxygen\ requirement} \quad (2)$$

where, $Oxygen_{fuel}$ and $Oxygen_{air}$ are considered the oxygen mass (wt%) in fuel and air respectively.

Table 2
Properties of test fuels (Nabi et al., 2009; Nabi and Hustad, 2010; Kannan et al., 2009).

Properties	Unit	Method	FT100	B25	B50	B75	B100
Density @15 °C	kg/m^3	EN3675	0.80	0.82	0.84	0.86	0.88
K. viscosity @40 °C	cSt	EN3104	2.81	3.01	3.24	3.46	3.70
Distillation temp. 90%	°C	ASTM D86	311	333	339	342	344
Flash point temp.	°C	EN3679	99	97	99	103	130
Cetane number	–	ASTM D613	52	54.6	57.8	61.9	65.8
Higher heating value	MJ/kg	ASTM D240	47.05	45.23*	43.4*	41.58	39.75
Lower heating value	MJ/kg	ASTM D4529	43.97	42.26*	40.55*	38.83*	37.12
Carbon (C)	wt%	ASTM D5291	85.5	83.10	80.7	78.4	76.3
Hydrogen (H)	wt%	ASTM D5291	14.5	13.89	13.4	12.9	12.4
Oxygen (O)	wt%	ASTM D5291	0	~3.0	5.9	8.7	11.3
Empirical formula	–	–	$C_{7.12}H_{14.39}$	$C_{6.91}H_{13.79}O_{0.188}$	$C_{6.72}H_{13.29}O_{0.37}$	$C_{6.53}H_{12.8}O_{0.544}$	$C_{6.35}H_{12.3}O_{0.706}$
C/H	–	–	5.90	5.97	6.03	6.07	6.15
H/C	–	–	0.169	0.167	0.165	0.164	0.162
O/C	–	–	0	0.0361	0.0731	0.110	0.148
S/C	–	–	<0.1	<0.1	<0.1	<0.1	<0.1

*Calculated.

2.3. Energy analysis

In the current investigation, the following assumptions were made for energy analysis (Odibi et al., 2019).

- The experimental engine system with the different components is taken as a control volume for the steady-state condition.
- The oxidation/combustion of fuel and air produce exhaust gas mixtures are considered ideal gas mixtures.
- Fuel, air and exhaust gas mixtures changes in kinetic and potential energies were considered as negligible.
- Fuels' lower heating value was used as the exhaust gases contain water vapour.

Based on the assumptions above, the input energy rate of fuel can be written as follows:

$$\dot{Q}_f = \dot{m}_f \times Lower\ heating\ value \tag{3}$$

where, $\dot{Q}_f$ is the fuel input energy rate (kW), and $\dot{m}_f$ is the fuel mass flow rate (kg/s).

The brake power, which is available in the shaft (W), can be estimated using Eq. (4).

$$W = \frac{2\pi NT}{60}\ (\text{kW}) \tag{4}$$

where, N is the speed in revolutions per minute and T: torque in kN m. The mass and energy balance for the control volume can be represented by Using the continuity equation, and the first law of thermodynamics, the mass and energy balance for the control volume can be written with Eqs. (5) and (6) respectively (Odibi et al., 2019).

$$\sum m_i = \sum m_e \tag{5}$$

$$\dot{Q}_{cv} - W = h_P - h_R \tag{6}$$

where, subscripts i, e, cv, P and R are inlet, exit states, control volume, product and reactant respectively.

The enthalpies of product and reactant (h_P, h_R) can be expressed using Eqs. (7) and (8), respectively.

$$h_P = \sum_P n_e(h_f^0 + \Delta\bar{h})_e \tag{7}$$

$$h_R = \sum_R n_i(h_f^0 + \Delta\bar{h})_i \tag{8}$$

where n is the number of moles and h_f^0 and Δh designate the standard enthalpy of formation and change of enthalpy with the change of state respectively. The standard enthalpy and the change of enthalpy at the exit temperature of the gases were taken from (Sonntag et al., 2003).

The enthalpy of formation of the reactant can be estimated using Eq. (9) from the complete combustion of fuel and theoretical air (Meisami et al., 2017).

$$C_xH_yO_z + (x + \frac{y}{4} - \frac{z}{2})(O_2 + 3.76N_2) \rightarrow xCO_2 + \frac{y}{2}H_2O + 3.76(x + \frac{y}{4} - \frac{z}{2})N_2 \tag{9}$$

Fuel standard enthalpy of formation can be found using the first law of thermodynamics using Eq. (10) (Odibi et al., 2019).

$$(h_f^0)_{Fuel} = x(h_f^0)_{CO_2} + 0.5y(h_f^0)_{H_2O} + (3.76x + 0.94y - 1.88z)(h_f^0)N_2 + \overline{Lower\ heating\ value} \tag{10}$$

The exhaust gases heat loss can be calculated as the difference between the rate of input energy from the air–fuel mixture, the shaft power (W) and the heat transfer as shown in Eq. (11) (Odibi et al., 2019).

$$\dot{Q}_{exh} = \dot{m}_f.lower\ heating\ value - (W + |\dot{Q}_{cv}|) \tag{11}$$

The brake thermal efficiency or energetic efficiency is defined as the ratio of shaft power ($W = \dot{E}_W$) and fuel input energy rate shown in Eq. (12) (Odibi et al., 2019).

$$Brake\ thermal\ or\ energetic\ efficiency = \frac{Shaft\ power}{Fuel\ input\ energy\ rate} = \frac{\dot{E}_W}{\dot{m}_f \times Lower\ heating\ value} \tag{12}$$

Like brake thermal or energetic efficiency, another engine performance parameter is the brake specific fuel consumption (BSFC). The BSFC is defined as the rate of fuel is needed to produce unit power in one hour. The BSFC is given by Eq. (13) (Odibi et al., 2019).

$$BSFC = \frac{\dot{m}_f}{W} \times 3600 \tag{13}$$

2.4. Exergy analysis

The assumptions made earlier for energy analysis are valid for exergy analysis. The reference environment temperature (T_0) in this investigation is taken as 298.15 K and an atmospheric pressure of 1 bar. The balance of exergy for the control volume is shown in Eq. (14) (Odibi et al., 2019).

$$\dot{E}_Q + \dot{E}_W = \sum \dot{m}_{in}e_{in} - \sum \dot{m}_{out}e_{out} - \dot{E}_{dest} \tag{14}$$

where $\dot{E}_Q$: the exergy flow rate accompanying heat leaving the control volume via the cooling water
$\dot{E}_W$: the exergy flow rate accompanying work
$\dot{E}_{dest}$: destruction exergy rate
$\sum \dot{m}_{in} e_{in}$: exergy rate (entering)
$\sum \dot{m}_{out} e_{out}$: exergy rate (exiting)
e_{in}: fuel specific exergy
e_{out}: exhaust gases specific exergy
$\dot{m}_{in}$: fuel mass flow rate
$\dot{m}_{out}$: exhaust gases mass flow rate

The exergy flow rate leaving the control volume through the cooling water is shown in Eq. (15) (Odibi et al., 2019).

$$\dot{E}_Q = \sum Q_{cv} \left(1 - \frac{T_0}{T_{cw}}\right) \tag{15}$$

where, T_0 and T_{cw} represent the temperatures of the reference environment and the cooling water, respectively.

The exergy flow accompanying work is the work available at the shaft. This is represented in Eq. (16) (Odibi et al., 2019).

$$\dot{E}_W = W \tag{16}$$

The input exergy rate is designated by Eq. (17) (Odibi et al., 2019).

$$\sum \dot{m}_{in} e_{in} = \dot{m}_f \, \phi |lower\ heating\ value| \tag{17}$$

where, ϕ is the chemical exergy factor and can be estimated using Eq. (18) (Odibi et al., 2019).

$$\phi = [1.0401 + 0.1728\frac{H}{C} + 0.0432\frac{O}{C} + 0.2169\frac{S}{C}(1 - 2.0628\frac{H}{C})] \tag{18}$$

where, H, C, O, and S are the mass fractions of hydrogen, carbon, oxygen and sulphur contents of the fuels listed in Table 2.

The exhaust gas exergies at a temperature T and pressure P can be shown in Eqs. (19) and (20) respectively (Kotas, 1995).

$$\sum \dot{m}_{out} e = \dot{n}_f (\bar{\bar{e}}_{tm} + \bar{\bar{e}}_{ch})$$

$$\bar{\bar{e}}_{tm} = \sum_i a_i [\bar{h}_{i,T} - \bar{h}_{i,T_0} - T_0 (\bar{S}^0_{i,T} - \bar{S}^0_{i,T_0})] + \bar{R} T_0 ln \frac{P}{P_0} \tag{19}$$

$$\bar{\bar{e}}_{ch} = \bar{R} T_0 \sum_i a_i \, ln \left(\frac{y_i}{y_{i,00}}\right) \tag{20}$$

where, a_i is the molar coefficient of i component. $\bar{H}$ and $\bar{S}$ stand for specific enthalpy and entropy of exhaust gases respectively, R is the gas constant, n designates the molar flow rate, To is the reference environment temperature, P and P_0 specify the exhaust gas pressure and reference environment pressure respectively. y_i represents the molar fraction of each gas component and $y_{i,00}$ shows the gas molar fraction in the reference environment (Table 3). The exhaust gas pressure is the same as atmospheric pressure. This is because the exhaust gases are discharged to the environment results in thermomechanical exergy to be zero. Different thermophysical properties of gases are obtained from (Sonntag et al., 2003).

The irreversibility related to the combustion process can be estimated using Eqs. (14)–(20). From Eq. (14), the destruction exergy can be mathematically written as:

$$\dot{E}_{dest} = \sum \dot{m}_{in} e_{in} - \sum \dot{m}_{out} e_{out} - \dot{E}_W - \dot{E}_Q \tag{21}$$

The analysis of different exergy components is important as those components give an idea of the fractions of exergy are taken away from input exergy. These fractions of exergy obtained from the combustion of fuel can be compared with other fuels whose heating values are different from the other fuel. It is important to estimate the fraction of the fuel exergy, which is converted to work. Second law efficiency, which is also known as exergetic efficiency (η_{exe}) deals with the fraction of the fuel exergy converted to the work. The second law efficiency or exergetic efficiency can be mathematically expressed in Eq. (22).

$$\eta_{exe} = \frac{\dot{E}_W}{\dot{E}_f} = \frac{\dot{E}_W}{\dot{m}_f \times \phi \times Lower\ heating\ value} \tag{22}$$

The internal combustion engine unitary exergetic cost is estimated with Eq. (23) (López et al., 2014).

$$Cost = \frac{\dot{E}_f}{\dot{E}_W} \tag{23}$$

Table 3
Definition of environment (Odibi et al., 2019).

Reference environment	Mole fraction
O_2	20.35
CO	0.0007
CO_2	0.0345
Others	0.91455
H_2O	3.03
N_2	75.67
SO_2	0.0002
H_2	0.00005

Table 4
Values of R^2 for different figures with four fuels.

Figure	R^2			
	FT100	B25	B50	B75
3a	0.997	0.998	0.999	0.992
3b	0.995	0.998	0.999	0.992
4a	0.861	0.892	0.843	0.815
4b	0.861	0.892	0.843	0.815
5a	0.999	0.999	0.996	1.000
5b	0.999	0.990	0.996	0.998
7	0.9972	0.9991	0.9995	0.9962
10	0.9969	0.9973	0.9972	0.9972
11	0.962	0.974	0.958	0.943
12	0.9999	1.000	1.000	0.9995
13	1.000	0.9999	0.9996	1.000

3. Results and discussions

This section illustrates the engine torque, fuel exergy rate, energy rate, combustion efficiency, exergetic efficiency, energetic efficiency, brake specific fuel consumption (BSFC) concerning oxygen ratio.

3.1. Fuel energy and exergy rate

In this study, the engine was run at five different torques (loads) including 50 N m, 400 N m, 800 N m, 1200 N m and 1450 N m respectively. According to Fig. 2a, engine torque of 50 N m corresponds to oxygen ratio of ∼17, 400 N m corresponds to ∼5.7, 800 N m corresponds to ∼ 3, 1200 N m corresponds to ∼2 and 1450 N m corresponds to ∼1.7. It is also to be noted that the engine torques of 50 N m, 400 N m, 800 N m, 1200 N m and 1450 N m correspond to 3%, 25%, 50%, 75% and 91% of the full load respectively. According to Fig. 2a the lower oxygen ratio associated with the higher engine load (higher torque in N m), and higher oxygen ratio associates with the lower engine load (lower torque in N m).

Fig. 2(b and c) indicate the fuel energy and exergy rate concerning oxygen ratio respectively, while Fig. 2d demonstrates the relationship between fuel exergy rate and energy rate. As can be seen from Fig. 2b, the fuel energy rate decreases as oxygen ratio increases. The energy rate is found to be higher at lower

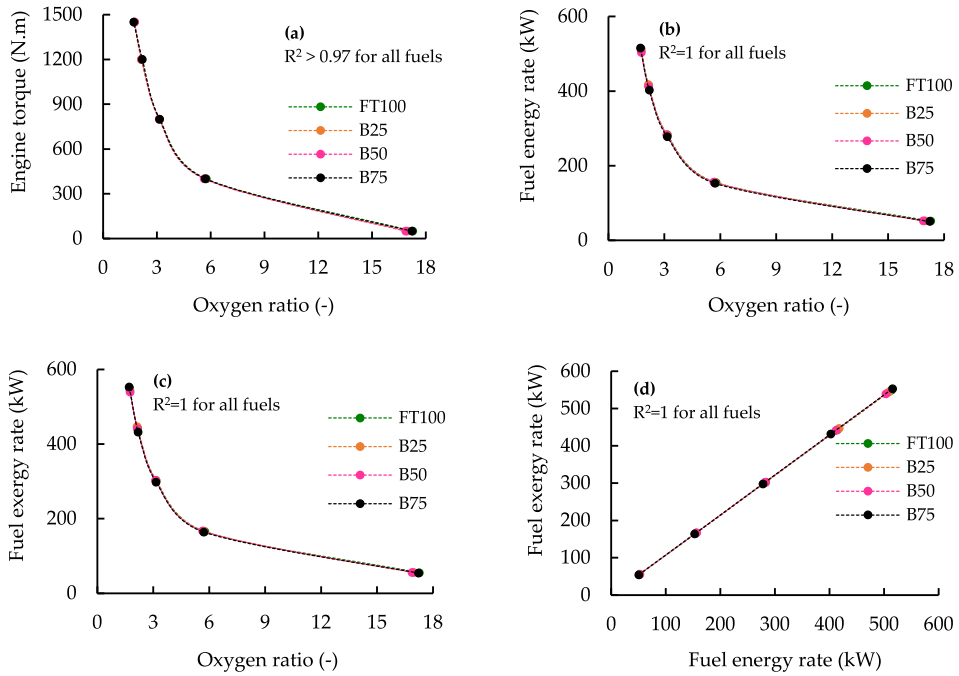

Fig. 2. Relationship between (a) engine torque against oxygen ratio, (b) fuel energy rate and oxygen ratio, (c) fuel exergy rate and oxygen ratio, (d) fuel energy rate and fuel exergy rate.

oxygen ratio. This is due to the higher amount of fuel is burned in the engine cylinder. It is interesting to note that all fuels show similar trends. A second-order polynomial analysis indicated an R^2 value of greater than 0.97, which shows a strong correlation between fuel energy rate and oxygen ratio. Similar trends of fuel energy rate to fuel energy rate were observed with all four fuels concerning fuel exergy rate and oxygen ratio with an R^2 value of unity indicating a strong correlation between fuel exergy and oxygen ratio. Absence or insignificant changes in fuel exergy rate concerning oxygen ratio were observed among the fuels. Fig. 2d illustrates a correlation between fuel exergy rate and energy rate. It is interesting to note that a linear correlation between those two parameters was observed with an R^2 value of unity.

The variations in energetic efficiency and exergetic efficiencies concerning oxygen ratio are depicted in Fig. 3a and b. Both efficiencies were computed using Eqs. (12) and (22), respectively. In general, for all fuels, the energetic and exergetic efficiencies decrease as oxygen ratio increases. The higher energetic and exergetic efficiencies were observed at higher engine loads that correspond to lower oxygen ratios, as seen in Fig. 3a and b. A close look at both Figures reveals that the exergetic efficiency (Fig. 3b) is lower than energetic efficiency for all fuels at all oxygen ratios. This is due to the denominator of Eq. (22) is higher than that of the Eq. (12). No significant variations of energetic or exergetic efficiencies were observed among all four fuels at five oxygen ratios, which are associated with five different engine loads. Fig. 3c depicts the variations of exergetic efficiency against energetic efficiency for the same four fuels at five different oxygen ratios. The regression analysis shows a linear correlation between exergetic and energetic efficiencies with an R^2 value of 1 except for B75, which shows the R^2 values of greater than 0.99 (Table 4).

The relationship between fuel energy rate and BSFC is displayed in Fig. 4a. Interesting to note that all fuels show almost similar energy rate with different BSFCs. It is clear from the Figure that for the energy rate of ∼507 kW (highest engine load), the BSFC for FT100 was observed to be 0.19 kg/kWh. For the same energy rate of ∼507 kW, the BSFCs for three oxygenated blends (B25, B50, B75) are found to be 0.20 g/kWh, 0.205 g/kWh and 0.21 g/kWh respectively. Similarly, for lowest engine load (energy rate: ∼52 kW), the BSFCs for FT100, B25, B50 and B75 were noted to be 0.56 g/kWh, 0.59 g/kWh, 0.61 g/kWh and 0.62 g/kWh. For all other three engine loads, the similar trends were observed. The second-order polynomial regression analysis indicates a good relationship between fuel energy rate and BSFC for all fuels with R^2 values of 0.815–0.892 (Table 4).

Fig. 4b illustrates the variations of fuel exergy rate against BSFC for all four fuels, including FT100, B25, B50 and B75. The exergy rate against BSFC displayed similar trends to energy rate, and BSFC were observed. However, the exergy rate shows higher than energy rate for all four fuels.

Fig. 5a and b demonstrate the variations of energetic and exergetic efficiencies against BSFC. As a whole, for all fuels, both energetic and exergetic efficiencies decrease as BSFC increases. It is evident from both Figs., BSFC decreased as engine load increases and found lowest at the highest load, where exergetic and energetic efficiencies are highest. FT100 shows the lowest BSFC while B75 shows the highest. It is also found that although the energetic and exergetic efficiencies do not show any significant differences among four fuels, higher BSFCs were observed with the oxygenated fuels compared to those of FT100. A second-order polynomial regression analyses show very high values of R^2 (>0.99, Table 4), indicating a strong relationship between energetic efficiency and BSFC as well as exergetic efficiency and BSFC.

Fig. 6 shows the changes in BSFCs with respect to oxygen ratio for FT100 and three oxygenated fuels. As illustrated in Fig. 6, the BSFCs are higher at higher oxygen ratios, which indicate lower engine loads. It is also seen from the Figure that all oxygenated fuels show higher BSFCs than FT100 at all loading conditions. The difference in BSFCs between FT100 and oxygenated fuels are higher for higher oxygen content blends, B75 in this case. This is associated with the lower heating values in higher oxygen content blends (refer to Table 2).

The variations in combustion efficiency against oxygen ratio are shown in Fig. 7. As can be seen from the Figure, combustion

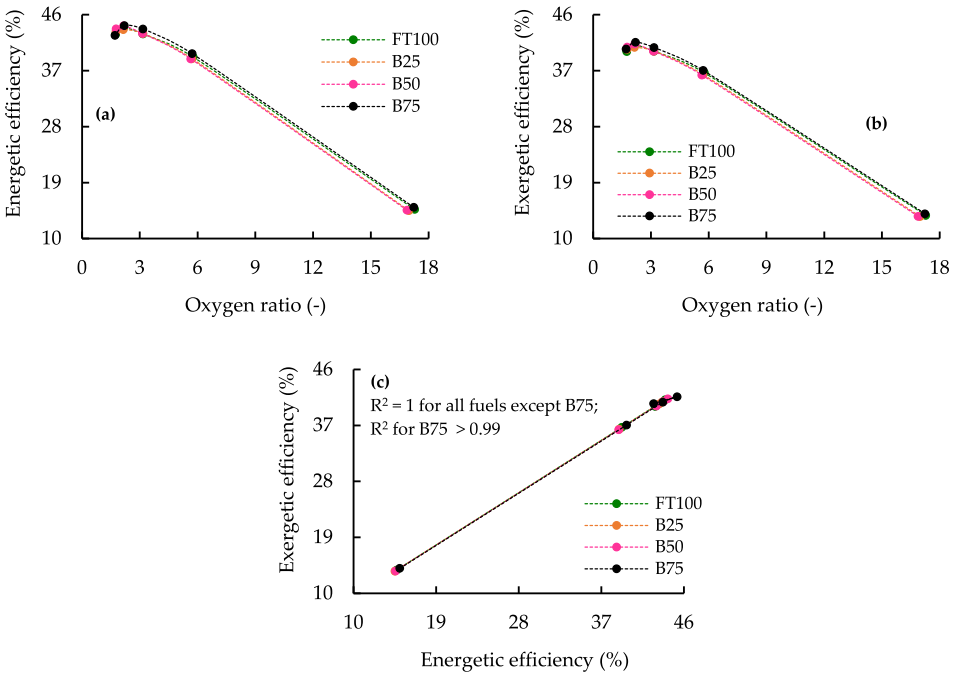

Fig. 3. Relationship between (a) fuel energetic efficiency and oxygen ratio, (b) fuel exergetic efficiency and oxygen ratio and (c) fuel energetic efficiency and fuel exergetic efficiency.

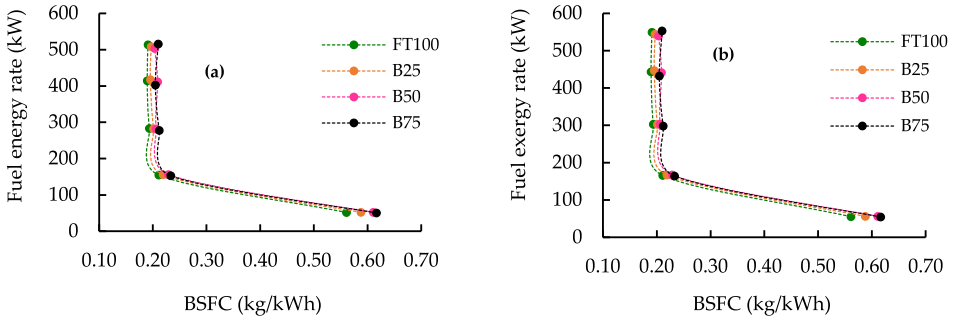

Fig. 4. Relationship between (a) fuel energy rate and BSFC, (b) fuel exergy rate and BSFC.

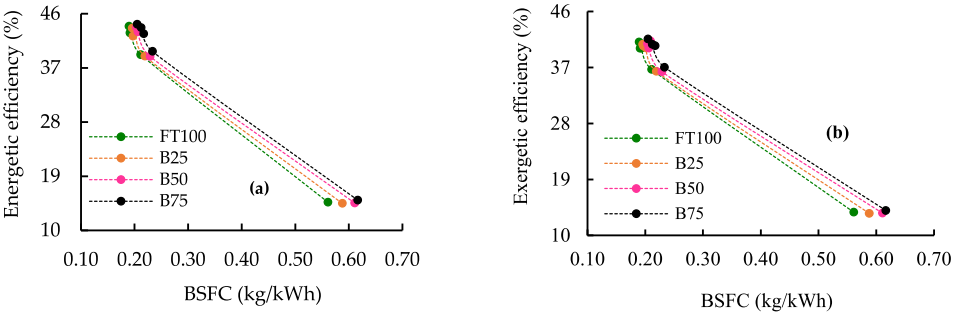

Fig. 5. Relationship between (a) fuel energetic efficiency and BSFC, (b) fuel exergetic efficiency and BSFC.

efficiency for all fuels increases with the increase in oxygen ratio. Insignificant variations in combustion efficiencies among the fuels were observed at all oxygen ratios. A second-order polynomial regression analysis indicates a strong correlation between combustion efficiency and oxygen ratio with an R^2 value of >0.99 for all fuels (refer to Table 4).

Figs. 8–9 show the destruction exergy versus oxygen ratio and destruction exergy versus BSFC, respectively, for the four fuels as explained in Figs. 1–7. As seen in Fig. 8, the destruction exergy

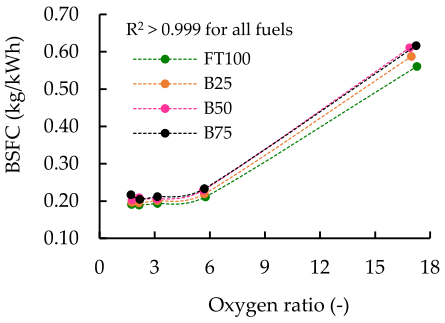

Fig. 6. Relationship between BSFC and oxygen ratio.

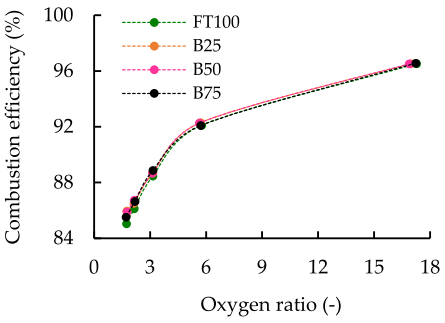

Fig. 7. Relationship between combustion efficiency and oxygen ratio.

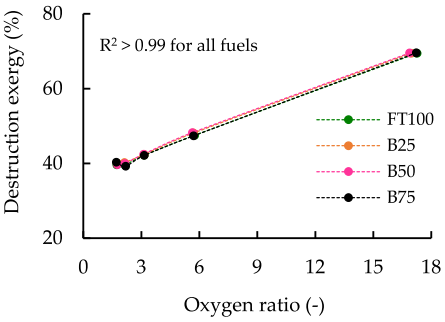

Fig. 8. Relationship between destruction exergy and oxygen ratio.

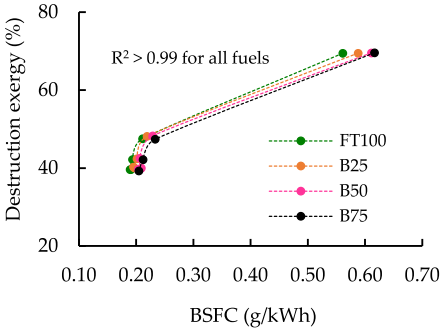

Fig. 9. Relationship between destruction exergy and BSFC.

is lower at lower oxygen ratio or higher at higher engine load for all four fuels. On the other hand, from Fig. 9, it is found that the destruction exergy gets lower at lower BSFC but higher at higher BSFC. Once again, it is revealed that the BSFCs are higher for three oxygenated blends compared to FT100 at all five oxygen ratios. From both Figures, the second-order polynomial regression analyses with an R^2 value of >0.99 show a strong correlation

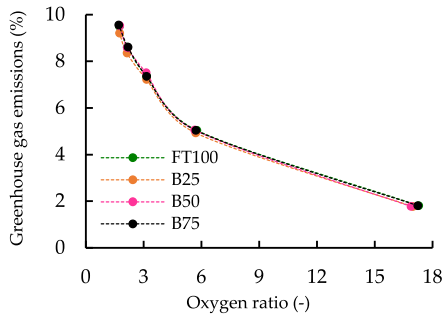

Fig. 10. Greenhouse gas emissions vs. oxygen ratio.

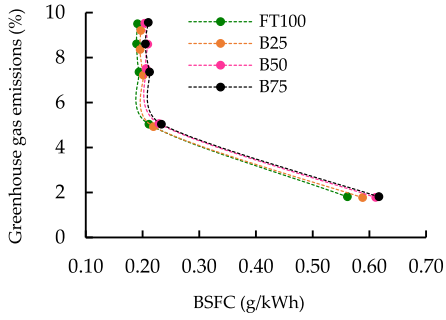

Fig. 11. Greenhouse gas emissions vs. BSFC.

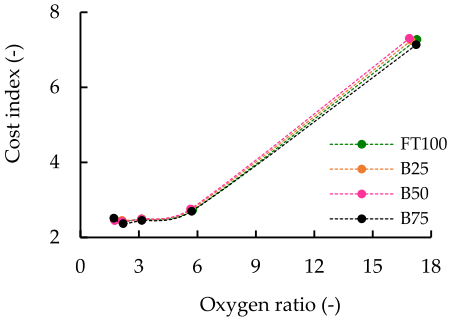

Fig. 12. Relationship between cost index and oxygen ratio.

between destruction exergy and oxygen ratio and destruction exergy and BSFC.

Figs. 10 and 11 demonstrate the variations of greenhouse (CO_2) gas emissions against oxygen ratio and greenhouse gas emissions against BSFC, respectively. As depicted in Fig. 10, the greenhouse gas emissions are higher at higher engine loads (lower oxygen ratios) but, lower at higher oxygen ratios or lower engine loads irrespective of the types of fuels. No significant changes in greenhouse gas emissions were observed among the oxygenated blends and FT100. From Fig. 11, greenhouse gas emissions decrease as BSFC increases for FT100 and all oxygenated blends. The good correlation between greenhouse gas emissions and oxygen ratio is displayed with a high R^2 value >0.99 (Table 4) for all fuels, while the R^2 values range from 0.94 to 0.97 (Table 4) for greenhouse gas emissions and BSFC correlation for the same four fuels. It is interesting to note that without deteriorating engine performance (results discussed in Figs. 2–9), the greenhouse gas emissions for the tested oxygenated blends show similar to those of reference FT100.

Figs. 12 and 13 show the relationship between unitary exergetic cost and oxygen ratio and unitary exergetic cost and BSFC for the same four fuels described in Figs. 1–11. The unitary

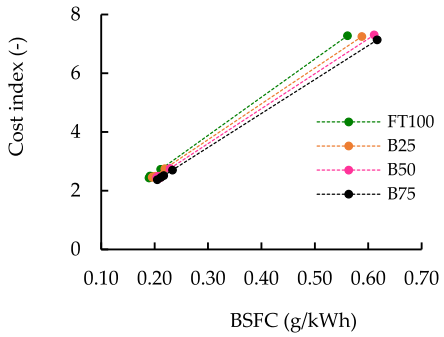

Fig. 13. Relationship between cost index and BSFC.

exergetic cost is estimated using Eq. (23). A close look at Eqs. (22) and (23) reveal that the exergetic efficiency and unitary cost are reciprocal to each other and Figs. 12 and 13 are exactly the inverse of Figs. 3b and 5b. The unitary exergetic cost (cost index in Figs. 12 and 13) signifies the least exergy of an internal combustion engine needs to yield one exergy unit of product (López et al., 2014). The unitary cost increases as oxygen ratio or BSFC increase. As seen from Figs. 12 and 13, there are no variations in unitary cost for oxygenated fuels compared to those of FT100 except at lower load condition (the extreme right points of Figs. 12 and 13). Introducing a new term "oxygen ratio" in this investigation shows a strong correlation with cost index with an R^2 value of >0.999 for all fuels. Similar results can be observed in Fig. 13, which shows insignificant changes in cost index with higher BSFCs for the oxygenated blends at all five engine loads. For all fuels, the R^2 values in Table 4 show close to unity, which indicates a very strong correlation between cost index and BSFC.

4. Conclusions

An experimental investigation with a series of Jatropha biodiesel blends (oxygenated fuels, B25, B50 and B75) along with a reference Fischer–Tropsch fuel (FT100) was conducted in a direct injection diesel engine. The results of this investigation are summarised as follows:

- The exergy and energy rates using three oxygenated blends are identical with those of reference FT100 fuel.
- The energetic and exergetic efficiencies with three oxygenated blends are identical compared to those of FT100.
- Relative to FT100, all three oxygenated blends show insignificant variations in destruction exergy at all engine loading conditions.
- The unitary exergetic cost (cost index) with oxygenated blends is found to be similar compared to FT100.
- When compared to base fuel FT100, the greenhouse gas (CO_2) emissions show no significant variations using three oxygenated blends.
- In all cases of the results and discussion section, the different energy, as well as exergy parameters and oxygen ratio, show a strong correlation between themselves with very high R^2 values.
- Considering the greenhouse gas emissions, cost index and different exergy and energy parameters, B25 could be considered as the potential candidate for diesel engine fuel. However, before using B25 in a diesel engine, further investigation is necessary to compare the current analytical analysis results with those of the modelling results.

Declaration of competing interest

The authors declare that they have no known competing financial interests or personal relationships that could have appeared to influence the work reported in this paper.

Acknowledgements

The authors thank Mr Ole Bergh, Marintek, Norway, for his help in this study. The authors also thank Dr Dhandapani Kannan of NTNU, Norway for his assistance during the experimental investigation.

References

Bodisco, T.A., Rahman, S.M.A., Hossain, F.M., Brown, R.J., 2019. On-road NOx emissions of a modern commercial light-duty diesel vehicle using a blend of tyre oil and diesel. Energy Rep. 5, 349–356.
Canakci, M., Hosoz, M., 2006. Energy and exergy analyses of a diesel engine fuelled with various biodiesels. Energy Sources, Part B: Econ. Plan. Policy 1, 379–394.
Hoseinpour, M., Sadrnia, H., Tabasizadeh, M., ghobadian, B., 2017. Energy and exergy analyses of a diesel engine fueled with diesel, biodiesel-diesel blend and gasoline fumigation. Energy 141, 2408–2420.
Iqbal, M.A., Varman, M., Hassan, M.H., Kalam, M.A., Hossain, S., Sayeed, I., 2015. Tailoring fuel properties using jatropha, palm and coconut biodiesel to improve CI engine performance and emission characteristics. J. Cleaner Prod. 101, 262–270.
Kannan, D., Nabi, M.N., Hustad, J.E., 2009. Investigation of fuel properties and characterization of new generation alternative fuel for diesel engine. In: Internal Combustion Engines: Performance, Fuel Economy and Emissions Conference. Institution of Mechanical Engineers, pp. 185–193.
Khoobbakht, G., Akram, A., Karimi, M., Najafi, G., 2016. Exergy and energy analysis of combustion of blended levels of biodiesel, ethanol and diesel fuel in a DI diesel engine. Appl. Therm. Eng. 99, 720–729.
Kotas, T., 1995. The Exergy Method of Thermal Plant Analysis. Krieger, Malabar, Florida.
Liu, H., Xu, J., Zheng, Z., Li, S., Yao, M., 2013. Effects of fuel properties on combustion and emissions under both conventional and low temperature combustion mode fueling 2, 5-dimethylfuran/diesel blends. Energy 62, 215–223.
López, I., Quintana, C.E., Ruiz, J.J., Cruz-Peragón, F., Dorado, M., 2014. Effect of the use of olive–pomace oil biodiesel/diesel fuel blends in a compression ignition engine: Preliminary exergy analysis. Energy Convers. Manage. 85, 227–233.
Meisami, F., Ajam, H., 2015. Energy, exergy and economic analysis of a Diesel engine fueled with castor oil biodiesel. Int. J. Engine Res. 16, 691–702.
Meisami, F., Ajam, H., Tabasizadeh, M., 2017. Thermo-economic analysis of diesel engine fueled with blended levels of waste cooking oil biodiesel in diesel fuel. Biofuels 9, 503–512.
Nabi, M.N., Akhter, M.S., Rahman, M.A., 2013. Waste transformer oil as an alternative fuel for diesel engine. Procedia Eng. 56, 401–406.
Nabi, M.N., Hustad, J.E., 2010. Influence of biodiesel addition to fischer–tropsch fuel on diesel engine performance and exhaust emissions. Energy Fuels 24, 2868–2874.
Nabi, M.N., Hustad, J.E., 2012. Influence of oxygenates on fine particle and regulated emissions from a diesel engine. Fuel 93, 181–188.
Nabi, M.N., Kannan, D., Hustad, J.E., 2009. Experimental Investigation of Diesel Combustion and Exhaust Emissions Fuelled with Fischer–Tropsch-Biodiesel Blends: Part-I. In: SAE TECHNICAL PAPER SERIES #2009-01-2721.
Nabi, M.N., Rahman, S.M.A., Bodisco, T.A., Rasul, M.G., Ristovski, Z.D., Brown, R.J., 2019a. Assessment of the use of a novel series of oxygenated fuels for a turbocharged diesel engine. J. Cleaner Prod. 217, 549–558.
Nabi, M.N., Rasul, M.G., 2018. Influence of second generation biodiesel on engine performance, emissions, energy and exergy parameters. Energy Convers. Manage. 169, 326–333.
Nabi, M.N., Rasul, M.G., Brown, R.J., 2019b. Influence of diglyme addition to diesel-biodiesel blends on notable reductions of particulate matter and number emissions. Fuel 253, 811–822.
Nabi, M.N., Rasul, M.G., Rahman, S.M.A., Dowell, A., Ristovski, Z.D., Brown, R.J., 2019c. Study of performance, combustion and emission characteristics of a common rail diesel engine with tea tree oil-diglyme blends. Energy 180, 216–228.
Odibi, C., Babaie, M., Zare, A., Nabi, M.N., Bodisco, T.A., Brown, R.J., 2019. Exergy analysis of a diesel engine with waste cooking biodiesel and triacetin. Energy Convers. Manage. (198).
Ozcan, H., 2010. Hydrogen enrichment effects on the second law analysis of a lean burn natural gas engine. Int. J. Hydrogen Energy 35, 1443–1452.

Panigrahi, N., Mohanty, M.K., Mishra, S.R., Mohanty, R.C., 2014. Performance, emission, energy, and exergy analysis of a C.I. Engine using mahua biodiesel blends with diesel. Int. Sch. Res. Noti. 2014, 207465.
Pham, P.X., Bodisco, T.A., Ristovski, Z.D., Brown, R.J., Masri, A.R., 2014. The influence of fatty acid methyl ester profiles on inter-cycle variability in a heavy duty compression ignition engine. Fuel 116, 140–150.
Rahman, M.M., Stevanovic, S., Islam, M.A., Heimann, K., Nabi, M.N., Thomas, G., Feng, B., Brown, R.J., Ristovski, Z.D., 2015. Particle emissions from microalgae biodiesel combustion and their relative oxidative potential. Environ. Sci. Process. Impact 17, 1601–1610.
Sayin Kul, B., Kahraman, A., 2016. Energy and exergy analyses of a diesel engine fuelled with biodiesel-diesel blends containing 5% bioethanol. Entropy 18.
Sonntag, R.E., Borgnakke, C., Van Wylen, G.J., Van Wyk, S., 2003. Fundamentals of Thermodynamics. Wiley New York, 2003.
Tat, M.E., 2011. Cetane number effect on the energetic and exergetic efficiency of a diesel engine fuelled with biodiesel. Fuel Process. Technol. 92, 1311–1321.
Zare, A., Bodisco, T.A., Nabi, M.N., Hossain, F.M., Rahman, M.M., Ristovski, Z.D., Brown, R.J., 2017. The influence of oxygenated fuels on transient and steady-state engine emissions. Energy 121, 841–853.
Zare, A., Nabi, M.N., Bodisco, T.A., Hossain, F.M., Rahman, M.M., Ristovski, Z.D., Brown, R.J., 2016. The effect of triacetin as a fuel additive to waste cooking biodiesel on engine performance and exhaust emissions. Fuel 182, 640–649.